We are IntechOpen,
the world's leading publisher of
Open Access books
Built by scientists, for scientists

6,900
Open access books available

186,000
International authors and editors

200M
Downloads

154
Countries delivered to

Our authors are among the

TOP 1%
most cited scientists

12.2%
Contributors from top 500 universities

CLARIVATE ANALYTICS
BOOK CITATION INDEX
INDEXED

WEB OF SCIENCE™

Selection of our books indexed in the Book Citation Index
in Web of Science™ Core Collection (BKCI)

Interested in publishing with us?
Contact book.department@intechopen.com

Could Coral Skeleton Oxygen Isotopic Fractionation be Controlled by Biology?

Anne Juillet-Leclerc

Abstract

During 1970s, coral skeleton oxygen isotope composition ($\delta^{18}O$) was regarded as the isotopic thermometer following thermodynamic rules. Recently, coral aragonite oxygen isotopic fractionation could appear to be controlled by biology, its rate being accelerated by an enzyme (carbonic anhydrase or CA). Such a new concept results of an original approach involving coral culture in controlled conditions. Environmental factors, temperature and also light have been tested on macrosize scale samples (some mg), and $\delta^{18}O$ revealed vital effects, anomalies compared with chemical and isotopic equilibrium, related to metabolic activity. $\delta^{18}O$ analyses at microsize scale (some μm), using ion microprobe, could display the mechanism of crystallisation, $\delta^{18}O$ fractionation responding to biological kinetic effects. The understanding of coral aragonite $\delta^{18}O$ is the absolute prerequisite to develop the first model of a coral proxy.

Keywords: oxygen isotopic fractionation, coral skeleton, culture, controlled conditions, temperature, light, organic matrix

1. Introduction

Coral colonies built the most important bioconstruction made of calcium carbonate ($CaCO_3$) of the world, with a calcification of about 2–6 kg_{CaCO3} m^{-2} $year^{-1}$ covering an area of about 284,300 km^2 [1]. This construction built from Jurassic results from the work of multiple small colonial organisms. The reefs, the biotic mound structure essentially made of corals as the Great Barrier Reef in Australia, are of major importance for marine ecosystems and biodiversity because they are the most productive and they host almost a third of all world fishes.

Corals are marine animals forming an aragonite (a polymorph of $CaCO_3$) skeleton. They are developed in two distinct ecosystems, essentially zooxanthellate corals or symbiotic ones living in shallow water and solitary colonies or integrated in elaborate reef framework in deeper depth than 50 until 2000 m. More than 793 coral species are spread over marine tropical zone [2]. Branched corals *Acropora* and massive corals *Porites* are ubiquitous genera [3]. We restricted this study to zooxanthellate corals.

Epstein [4, 5] demonstrated that skeletal carbonates of marine shells display similar oxygen isotopic composition ($\delta^{18}O_{CaCO3}$) relationship versus SST than inorganic calcium carbonate ($CaCO_3$) deposited from seawater at the same temperature, following thermodynamic laws.

$$\delta^{18}O = \left\{ \left[\left({}^{18}O / {}^{16}O \right)_{sample} / \left({}^{18}O / {}^{16}O \right)_{standard} \right] - 1 \right\} * 10^{-3}$$

The relationship was expressed as:

$$SST{}^{\circ}C = 16.5 - 4.3 \left(\delta^{18}O_{CaCO_3} - \delta^{18}O_{seawater} \right) + 0.14 \left(\delta^{18}O_{CaCO_3} - \delta^{18}O_{seawater} \right)^2 \quad (1)$$

from [5] with sea surface temperature (SST) being sea surface temperature and $\delta^{18}O_{seawater}$ seawater isotopic composition. The authors underlined that coral skeleton presented poor interest [4].

However, after preliminary studies [6], Weber and Woodhead deduced, despite apparent isotopic disequilibrium between coral skeletal carbonate and ambient seawater, that $\delta^{18}O_{coral}$ was temperature dependent. To support this assumption [2], the authors conducted isotopic analyses of coral skeleton collected over wide range of temperatures. This data series still constitutes the most exhaustive oxygen isotopic database existing for corals. Weber and Woodhead concluded that the calibration between annual $\delta^{18}O$ and annual SST differed following each coral genus, and the isotopic disequilibrium was attributed to vital effect, anomalies compared with chemical and isotopic equilibrium, related to metabolic activity. Several models of mineralisation were proposed to explain the geochemical specificities of coral skeletons based on kinetic fractionation [7–9] disturbed by "vital effects". Other models, based on precipitation efficiency [10] or Rayleigh fractionation [11–13], were suggested.

We developed drastically different approach considering that corals are animals living in symbiosis with algae, building aragonitic skeleton intimately related to biological activity. In collaboration with biologists from CSM (Centre Scientific de Monaco), Stéphanie Reynaud and Christine Ferrier-Pagès, and Claire Rollion-Bard geochemist from IPGP (Institut Physique du Globe de Paris), we developed an innovative strategy on cultured *Acropora* to identify what was hidden under the term of vital effect of coral skeleton and to highlight the isotopic fractionation involved in. We focused our study on the stable oxygen isotopic ratio $\delta^{18}O$. Branched coral *Acropora* and massive ones *Porites* belong to different genera but responses to environmental forcing in terms of biological parameters and isotopic signatures are regarded as similar.

Our demonstration is structured as followed: first, the main coral features are highlighted; second, we describe coral culture proceeding; third, temperature and light test results are presented at microscopic size scale; and finally, we display the stable oxygen isotopic ratio $\delta^{18}O$ as indicator of deposit mechanism.

2. Main coral features

Shallow corals, because they are leaving in symbiosis with micro algae need light to benefit from photosynthetic activity.

2.1 Notions of coral morphology and biological activity

Coral skeleton is extracellular, located at the base of coral tissue, constituted of similar units, the polyps. Each polyp looks like a bag made by two layers of cells (**Figure 1**). Polyps are linked together by the coenosarc. Most of zooxanthellae are located within an internal layer (**Figure 1**).

Biological activity might be quantified. Photosynthesis and respiration were measured using the respirometry technique, which measured the changes in oxygen concentration at different light levels. Rates of net photosynthesis and respiration
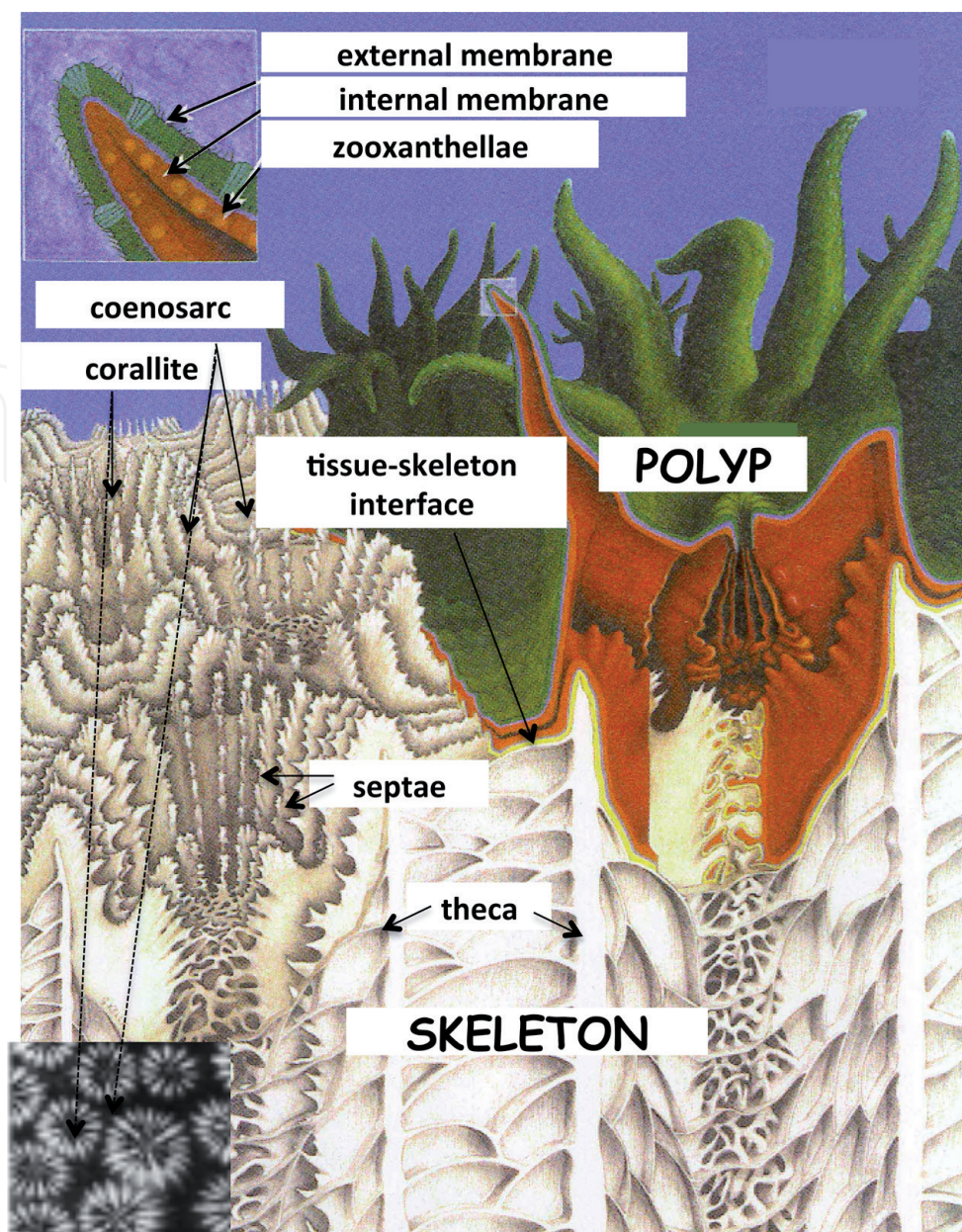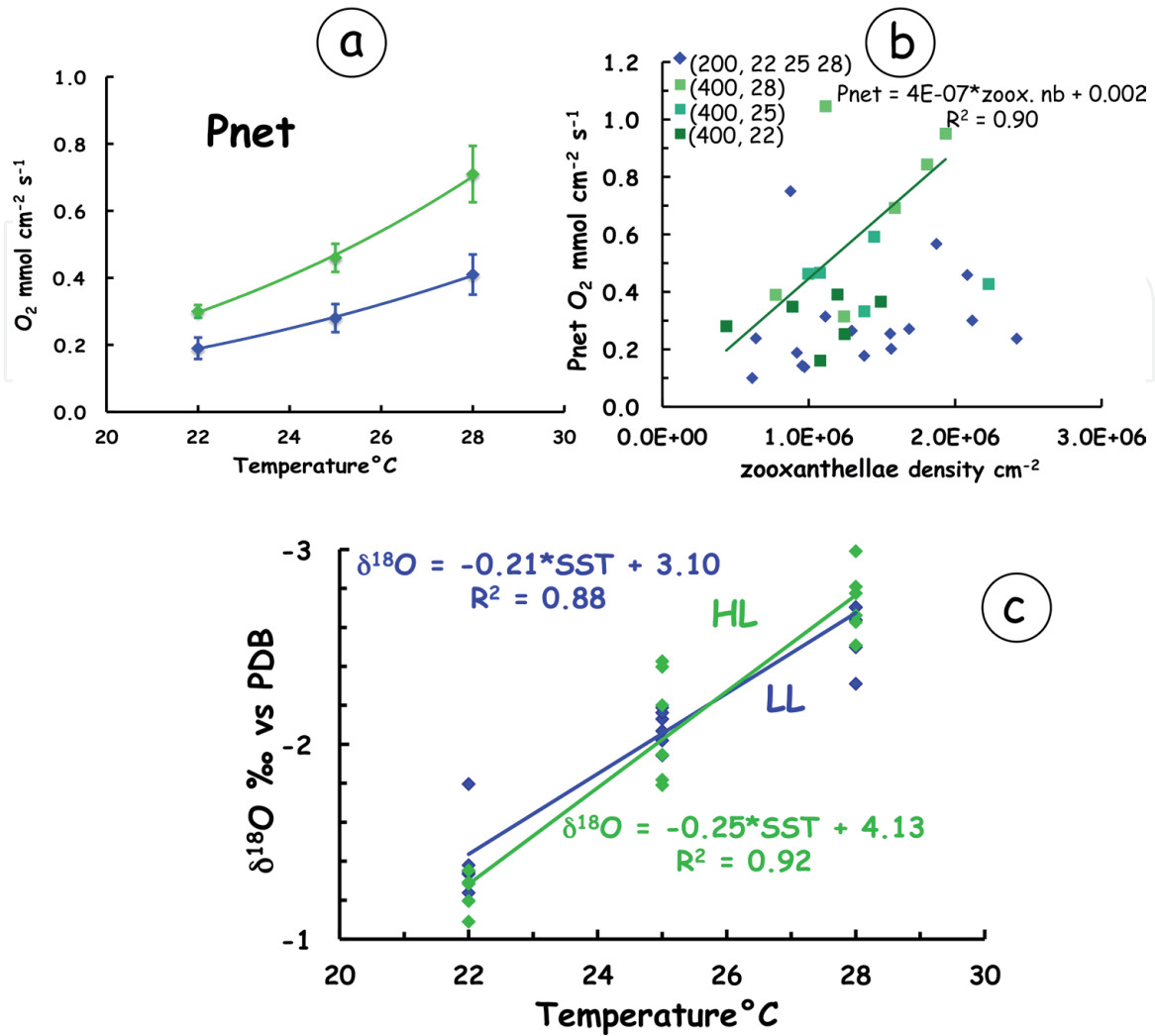
Figure 1.
Organisation of the coral adapted from [14]. The colour polyp is the living organism, an animal building the white skeleton. The animal lives in symbiosis with algae, the zooxanthellae, located in the internal layer (the left side high corner). A detail of mesoscale skeletal architecture figures on the left side bottom corner.

were estimated using a linear regression of O_2 against time [15]. By using two light intensities, at three temperatures (**Figure 2**), it appeared that increasing temperature enhanced photosynthetic activity, the effect arising with light intensity (**Figure 2a**) [15]. Additionally, coral growth rates might be estimated. Corals were weighed regularly using the buoyant weight technique and the surface expansion of the new skeleton formed was estimated [15]. It was generally accepted that calcification was light-enhanced (LEC or light enhanced calcification) during the day [16]. Zooxanthellae density and pigment concentration were determined under the light microscope using a counting chamber [15]. Coral symbiont distribution was not homogeneous on the skeleton and it differed following different coral genera, different depths in the fields. For example, tips of coral branches or other exposed surfaces were sun-adapted while most of the lowest parts were shade-adapted [15]. Iluz and Dubinsky [17] listed all the strategies developed by coral to optimise the light impinging on the zooxanthellae.

Measures at millimeter scale

Figure 2.
Test using a factorial design of three temperatures (22, 25, and 28°C) and two light intensities (200 and 400 μmol photon $m^{-2} s^{-1}$) of cultured Acropora. *Biologic response of net productivity (a), zooxanthellae density according to net productivity (b) and averaged δ^{18}O-temperature calibration under high light (HL) and low light (LL) (c).*

2.2 Microstructures of coral skeletal

It was admitted that the coral skeleton such as coral *Acropora* (**Figure 3a** and **b**) or coral *Porites* presented composite mineral microstructures: centres of calcification (COC) and fibres, embedded in a few organic matter as a network [18]. COC were massive randomly oriented crystals called fusiform crystals (**Figure 3c, h** and **i**) [19], and numerous needle-like crystals projecting in many directions from the fusiform crystals were called the fibres gathered into bundles (**Figure 3e, f** and **g**) [19] oriented perpendicularly to the growth axis (**Figure 3e**) [19].

Skeletogenesis could be the result of two different processes: the deposition of fusiform crystals and the progressive thickening of the initial framework by needle like crystals (**Figure 3f**) [19].

These crystalline elements were differently distributed according to morphology [19–21]. Each microstructure is preferentially present in some morphological parts, which were more or less developed following the genus [22]. However, we know that they are composed by identical microstructures and only differ by their relative amounts.
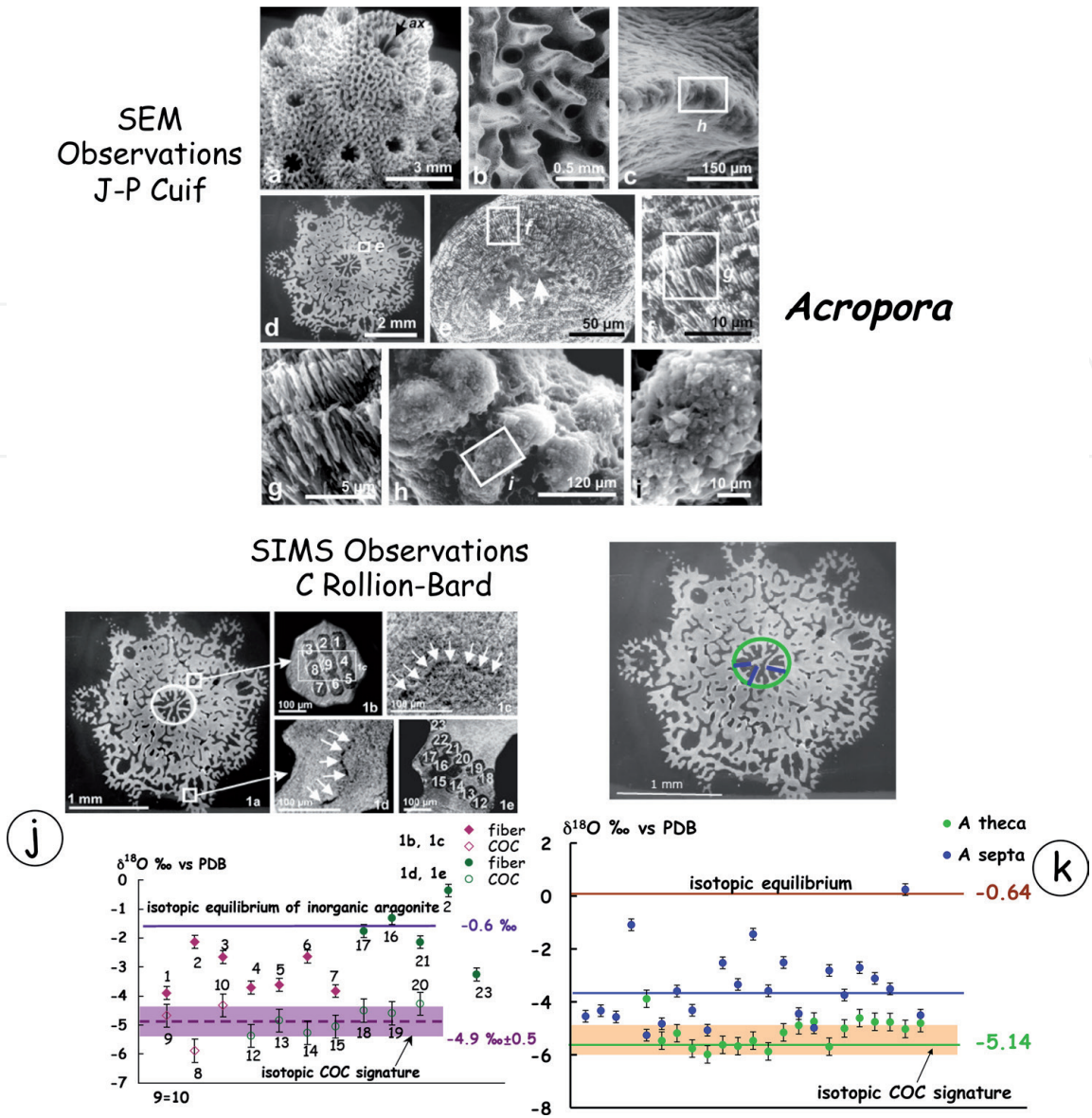
Figure 3.
Identification of mineralisation mechanism of microstructures COCs and fibres using microscopic $\delta^{18}O$ analyses. SEM observations of cultured Acropora *microstructures (a–i). microstructure identification and isotopic signatures (j). COC and fibre location on theca and septa from cultured* Acropora *(k).*

2.3 Consequences on $\delta^{18}O$

The oxygen isotopic composition of coral skeleton was measured on conventional spectrometer at mm size scale and might be also measured at micrometre scale by using ion microprobe.

Coral skeleton $\delta^{18}O$ was impacted by biology, which was essentially responsible of the vital effect. Most of the models proposed by geochemists neglect biology effects on $\delta^{18}O$, isotopic fractionation only depending on seasurface temperature and isotopic composition, $\delta^{18}O_{seawater}$ following Eq. (1). All climate reconstructions are derived according to this rule, including the estimate of both temperature and salinity based on the use of paired $\delta^{18}O$ and Sr/Ca measured on the same sample [23–25]. Salinity values deduced by this method are systematically misleading, d18O and Sr/Ca SST calibrations being based on classical thermodynamics. Whereas consequences of temperature and light on coral growth rates is well known by biologists [26], light effect is ignored by geochemists because the demonstration of this influence cannot be established from field data and needs culture tests.

$\delta^{18}O$ differed following microstructures at microscopic size scale (**Figure 3j** and **k**) [27]. This was confirmed later on [28, 29]. COC $\delta^{18}O$ was lower, while fibre $\delta^{18}O$ was higher and variable between equilibrium and COC value (**Figure 3j** and **k**) [29].

3. Calibrations of annual and monthly $\delta^{18}O$-temperature

3.1 Weber and Woodhead (1972) data set and annual calibrations revisited

Weber and Woodhead [3] established a formula able to predict past SST following the isotopic thermometer concept [30], expressed as:

$$SST°C = a \times \delta^{18}O\ (‰) + b \qquad (2)$$

(a) and (b) being constants (instead of A and B in [3]).

Because *Acropora* and *Porites* are ubiquitous genera, *Acropora* and *Porites* $\delta^{18}O$ calibration deriving from 835 and 421 sample, respectively, calibrations (**Figure 4a** and **b**) might be regarded as statistically significant. Moreover, isotopic analyses were conducted on annual samples, identified by X-ray growth bands, a pair of clear and dark bands corresponding to the annual growth [31]. Each temperature
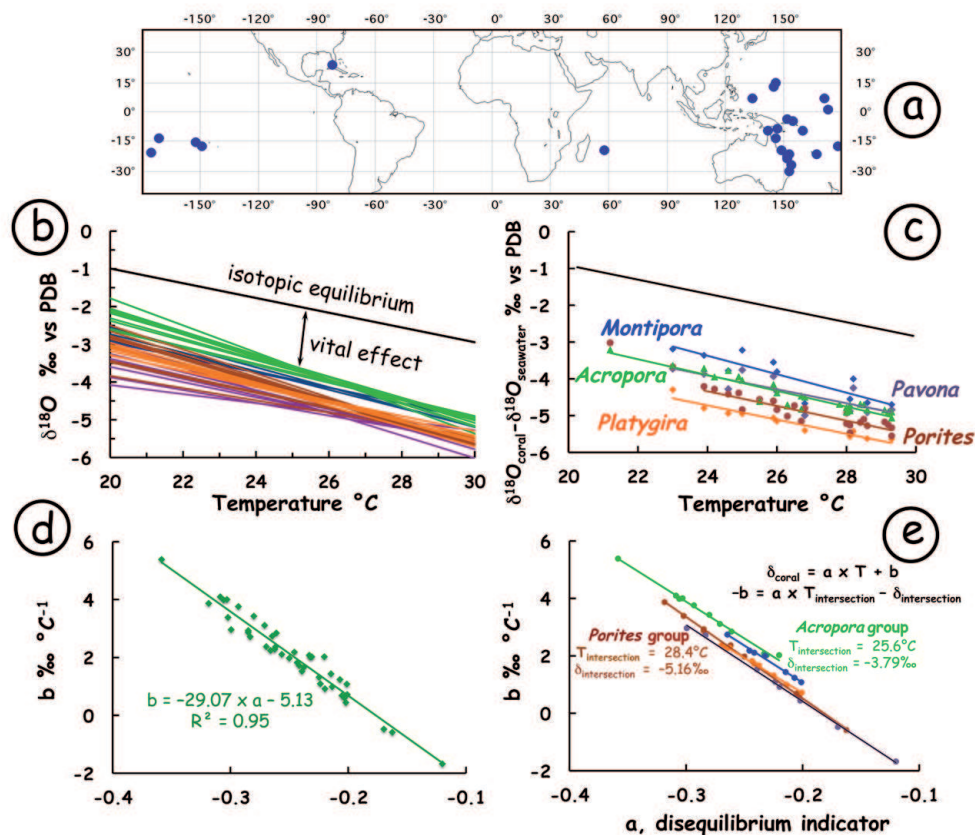

Figure 4.
Annual coral $\delta^{18}O$ measures performed on several genera from revisited dataset of [3] (a–e). Location of the 29 sites where coral samples were collected, prescribing temperature values (a). Calibrations of 44 coral genera following $\delta^{18}O(‰) = a \times SST°C + B$ (b). The colours highlight genera sharing identical temperature and isotopic ranges, underlining the convergence of the groups including Acropora *and* Porites. *Calibrations of some coral genera* Acropora, Porites, Platygira, Montipora *or* Pavona *following $\delta^{18}O_{carbonate} - \delta^{18}O_{seawater} = a \times \delta^{18}O(‰) + b$ (c). The colours of the calibrations correspond with colours from (c). strongly significant linear relationship linking constants a and b, of annual $\delta^{18}O$-annual temperature calibrations for 44 coral genera (d). Strongly significant linear relationship linking constant of annual $\delta^{18}O$-annual temperature calibrations for groups highlighted on (c and e).*

value, corresponding to one island, as associated to the averaged $\delta^{18}O$ measured for corals of the same species, all receiving identical local irradiation. Groups of genera including *Acropora* or *Porites* displayed strong convergence.

The dataset [3] did not take into account $\delta^{18}O_{seawater}$. Juillet-Leclerc and Schmidt [32] included annual $\delta^{18}O_{seawater}$ values assessed in the calibration established for *Porites* following the formula:

$$\delta^{18}O_{carbonate} - \delta^{18}O_{seawater} = -0.20 \times SST\ (°C) + 0.45 \quad (3)$$

with $R^2 = 0.83$, N = 22, $p < 0.001$, only significant over the SST range from 24 to 30°C [32].

However, the correlation linking $\delta^{18}O$ directly to temperature showed a higher coefficient [3]:

$$\delta^{18}O_{carbonate} = -0.27 \times SST\ (°C) + 2.24 \quad (4)$$

with $R^2 = 0.91$, N = 24, $p < 0.001$ including the lowest temperatures neglected in Eq. (5) [32].

A similar procedure was conducted for *Acropora*, using the same $\delta^{18}O_{seawater}$. We obtained:

$$\delta^{18}O_{carbonate} - \delta^{18}O_{seawater} = -0.21 \times SST\ (°C) + 1.26 \quad (5)$$

with $R^2 = 0.87$, N = 24, $p < 0.001$, significant over the temperature range from 21 to 30°C (**Figure 4e**).

the correlation linking $\delta^{18}O$ directly to temperature showed a higher coefficient [3]:

$$\delta^{18}O_{carbonate} = -0.28 \times SST\ (°C) + 3.34 \quad (6)$$

with $R^2 = 0.98$, N = 27, $p < 0.001$, significant over the temperature range from 21 to 30°C.

Slopes (a) shown by *Porites* and *Acropora* temperature calibrations including $\delta^{18}O_{seawater}$, −0.20 and −0.21‰/°C, respectively, differed from those deriving only from $\delta^{18}O_{carbonate}$ (referred as $\delta^{18}O$ in the following) and temperature. They were close to the slope of −0.19‰/°C assessed for inorganic aragonite calibration [33]. Slopes have been also obtained from other genera such as *Platygira*, *Montipora* or *Pavona* (**Figure 4e**) [3].

After introducing $\delta^{18}O_{seawater}$ into dataset [3], for *Porites* and *Acropora* genera, the usual thermodynamic equation is significant but to a lower degree, compared to Eqs. (4) and (6). For example, by taking into account only temperature, $R^2 = 0.91$ and 0.98 instead of 0.87 and 0.93 for *Porites* and *Acropora* respectively.

In the calibrations depending only on temperature, temperature might act first, according to thermodynamic law [5, 15] and second, through the photosynthetic process [34] (**Figure 2a**), which was enhanced by a temperature increase. Therefore, an increase in temperature induced a decrease in $\delta^{18}O$ following the first process while the second mechanism caused a rise in $\delta^{18}O$, confusing the global isotopic effect. Temperature influences $\delta^{18}O$ twice, explaining that temperature is the main factor, which does not exclude the role of $\delta^{18}O_{seawater}$.

Calibrations taking into account $\delta^{18}O_{seawater}$ exhibited a slope value close to isotopic equilibrium of inorganic aragonite with water, suggesting that under quasi-uniform light, the isotopic offset of coral $\delta^{18}O$ is constant, regardless of temperature (**Figure 4c**). Eqs. (3) and (4) confirm that, to a lesser degree than temperature, $\delta^{18}O_{seawater}$ may be included in a calibration.

When comparing constants (a) and (b) of Eq. (2) from data series [3], for all genera annual $\delta^{18}O$-annual temperature calibrations (**Figure 4d**), we obtained a strongly significant linear relationship:

$$b = -29.07 \times a - 5.13 \qquad (7)$$

with $R^2 = 0.95$, $N = 37$ and $p < 0.001$. (a) corresponds to a disequilibrium indicator compared to -0.19, the slope value derived from the theoretical $\delta^{18}O$ at equilibrium [34]. Such a relationship was not hazardous, but reflected inherent features of annual $\delta^{18}O$-annual SST calibrations. Linear calibrations determined from single genus deduced from figures or table of [3], showed strong correlation coefficients: $R^2 = 0.99$ (**Figure 4e**).

This suggests that the $\delta^{18}O$ SST dependence is based on a unique rationale according to taxonomy, in turn inherent to the coral skeleton.

Dataset [3] revealed unique relationship between annual $\delta^{18}O$-annual temperature calibrations of each genus, because coral taxonomy is based on morphology. Land et al. [22] stressed the high $\delta^{18}O$ variability following the longitudinal section on the calices of some species or the septa dentations of another one, inducing that according to coral morphology, some skeleton portions might be more or less developed, implying a large isotopic variability.

We underlined the relationship existing between the annual $\delta^{18}O$-annual SST calibration constants. However, identical feature was highlighted for annual Sr/Ca-annual temperature calibrations [35–37]. The link existing between $\delta^{18}O$ and Sr/Ca is not straightforward, oxygen being a component of $CaCO_3$ and Sr/Ca an impurity included in the skeleton. However, it is possible to recognise common $\delta^{18}O$ and Sr/Ca behaviour relative to their microstructure distribution in the coral and the concept of taxonomy.

Coral skeleton presents composite mineral microstructures: centres of calcification (COC) and fibres, embedded in a few organic matter as a network [18], differently distributed according to morphology [19–21]. Latter authors show that COC and fibres are essentially present in morphological parts, more or less developed following the genus. On the one hand, $\delta^{18}O$ signature differs according to the microstructures [19–21], COC $\delta^{18}O$ being lower than fibre $\delta^{18}O$ [29] (**Figure 3j** and **k**). On the other hand, Sr/Ca ratios measured on COCs are higher than those of fibres [9]. Cohen et al. [37] examined synchronously deposited microstructures on *Porites lutea* over a year, exhibiting COC elemental ratios systematically higher compared to those of fibres developed over an identical period. Thus, it is the proof that annual COC Sr/Ca value is higher than the annual fibre Sr/Ca signature [37]. Therefore, we suggested that discrepancies of morphology existing between coral genera are due to differences of microstructure proportions [22], explaining common features between the annual trace element ratio- and annual $\delta^{18}O$-annual temperature calibrations.

3.2 Identification of microstructures and their isotopic signatures using microsensor

Several small colonies of *Acropora verweyi* (Archaeocoeniina) were cultured following the procedure described by Reynaud-Vaganay et al. [38] under constant and controlled conditions, in Centre Scientific of Monaco (CSM) (**Figure 5**). Such colonies grew glued onto glass slides (**Figure 5**). Morphology of the microstructures, using on a scanning electron microscope (SEM Philips 505) was similar to observations performed by Cuif and Dauphin [19] (**Figure 3a–i**).
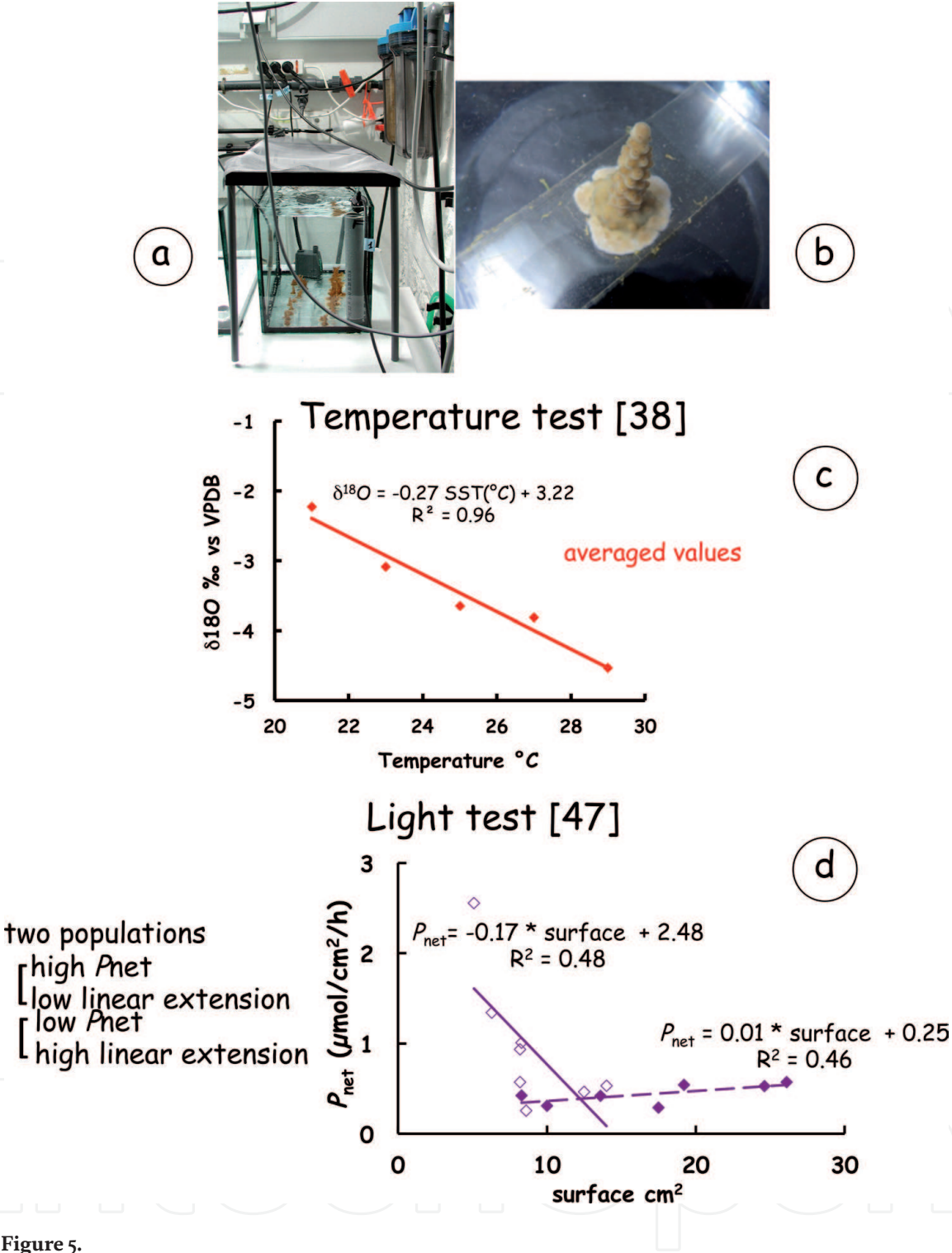
a

b

Temperature test [38]

c

$\delta^{18}O = -0.27\ SST(°C) + 3.22$
$R^2 = 0.96$

averaged values

δ18O ‰ vs VPDB

Temperature °C

Light test [47]

d

two populations
⌈high Pnet
⌊low linear extension
⌈low Pnet
⌊high linear extension

$P_{net} = -0.17 * surface + 2.48$
$R^2 = 0.48$

$P_{net} = 0.01 * surface + 0.25$
$R^2 = 0.46$

P_{net} (µmol/cm²/h)

surface cm²

Figure 5.
Culture experiment (a and b) to test $\delta^{18}O$ variability caused separately by temperature (c) and by light (d). Aquarium in CSM (a) coral Acropora *glued on glass slide showing new formed aragonite both on the colony surface and on the glass slide (b). $\delta^{18}O$-temperature calibration derived from averaged isotopic measures (c). Relationship between Pnet and linear extension, revealing the partition of colonies into two populations, following potential photosynthetic response of colonies (d).*

The new skeleton, formed under unique controlled condition, was grown on the glass slide, and sampled for the calibration of the growth units (**Figure 3j**). COC- and fibre-enriched zones were identified using SEM [29]. To characterise separately the isotopic signature of fibres and COC, analyses were focused on the microstructures earlier identified on the newly formed skeleton on two zones (**Figure 3a–c**; **Figure 3j**). We then focused our measurements around the theca of the newly formed skeleton (**Figure 3k**) where Gladfelter [39] recognised large amounts of "fusiform crystals" (**Figure 3e**). The sampling of the septae aimed

at confirming the presence of both COC and fibres as they have been identified from SEM observations [26].

The present study, confirmed that there was a strong relationship between isotopic value, crystal shape and skeleton morphology [29]. Crystals called "fusiform" by Gladfelter [39], according to their shape, show the same isotopic values as COC. We distinguished in septa both COC and fibres (**Figure 3k**). This confirmed microscopic observations of septa [21] showing discontinuous COC surrounded by fibres.

Isotopic fractionation was likely of kinetic origin, the rate changing according to microstructure. Skeleton microstructures $\delta^{18}O$ shed in light how chemical and/or physical processes might be adapted by biology to form crystals characterised by specific shapes and distributed following a hierarchical arrangement. The present study demonstrated that the presence of organic molecules (the organic matrix located at the interface tissue-mineral (**Figure 1**) had the capability to control the mineral deposition mechanism. Probably, the influence of external factors should be superimposed on the chemical signature of coral biomineral genetically determined).

3.3 Monthly calibrations on coral *Porites*

The preliminary step of climatic reconstruction using *Porites* skeleton, the genus more often analysed in this context, consisted of the assessment of seasonal $\delta^{18}O$-seasonal temperature calibration based on monthly instrumental temperatures over the last decades covered by the core. Sampling was conducted along the coral's growth through time, following the maximal growth rate perpendicular to the annual density bands shown by X-ray [40].

At millimetre size scale, it was also possible to highlight the strongly significant linear relationship between the constants of seasonal $\delta^{18}O$-seasonal temperature calibrations and to relate behaviour of the constants of the seasonal-$\delta^{18}O$- and Sr/Ca-seasonal temperature calibrations to the presence of two crystallographic units. Following DeLong et al. [40], fibres insuring the thickening of a colony should be preferentially deposited during a less active photosynthesis, whereas COC insuring axial growth should be formed during high photosynthetic activity. Juillet-Leclerc and Reynaud agreed, however, they demonstrated that growth mode was not so simple [34].

In order to test seasonal $\delta^{18}O$-seasonal temperature calibration variability including the seasonal light effect, calculated for several coral cores collected on a given site, at different temperature ranges, we considered studies conducted on several *Porites* colonies from three sites. The mean annual temperature offshore Amédée Island, New Caledonia (22°29′ S, 166°28′ E) was 24.72°C, over the period 1968–1992 [41, 42], while at Clipperton Atoll (10°18′ N, 109°13′ W) the mean annual temperature was 28.5°C, over the period 1985–1995 [43] and in the Flores Sea, Indonesia (6°32′ S, 121°13′ E) the mean annual temperature was above 28°C, over the period 1979–1985 [44].

We assumed that calibrations measured on different coral colonies grown at a given site (New Caledonia, Clipperton or Indonesia) differed according to various light sensitivities due to depth or light incidence or acclimation because seasonality strongly affected light variations, and was likely different following site location (**Figure 6a**). However, calibration constants calculated from monthly data for *Porites* remained strongly correlated (**Figure 6b**) as we previously observed for annual $\delta^{18}O$-annual temperature calibrations.

As seasonal $\delta^{18}O$-seasonal temperature calibrations presented similar behaviours, even in different sites characterised by distinct $\delta^{18}O_{seawater}$, they did not reflect classical thermodynamics.

Seasonal $\delta^{18}O$ of *Porites* [41-44]

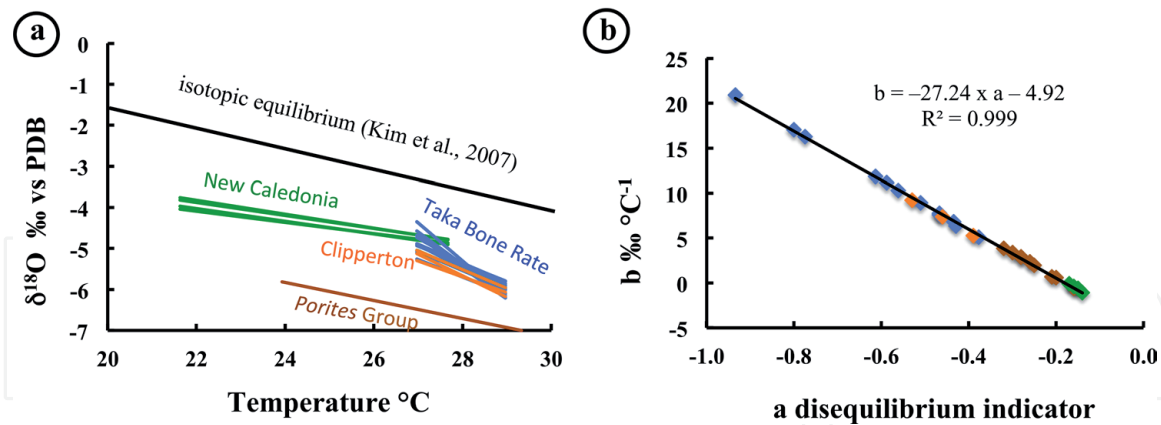**Figure 6.**
Porites monthly $\delta^{18}O$ from [41–44] (a and b). Monthly $\delta^{18}O$-monthly temperature calibrations for coral Porites *and annual $\delta^{18}O$-annual temperature for* Porites *group as defined in* **Figure 4c** *(a) and associated constant relationship (b).*

4. Coral cultures simulating different environmental conditions

4.1 Test of temperature

New technique of culture was developed to calculate $\delta^{18}O$-temperature calibration for *Acropora sp*. The experiment was conducted in Centre Scientific of Monaco (CSM) using colonies of the branching zooxanthellate scleractinian coral, *Acropora sp*. (**Figure 5a** and **b**), in the Gulf of Aqaba (1 m depth) [38]. The nubbins (new colony fragments) were collected from unique parent colony. The specimens were glued on glass slides. Chemical conditions were kept constant during the experiment, as $\delta^{18}O_{seawater}$ (1.29 ± 0.01‰ vs. SMOW) measured in the aquaria under light (260 µmol m^{-2} s^{-1}) on a 12:12 h photoperiod [38]. Five temperatures were tested on six coral fragments. The skeletal powder was treated following the method described by Boiseau and Juillet-Leclerc [45].

The calibration given by the experiment (**Figure 5c**) might be expressed as:

$$\delta^{18}O_{coral} - \delta^{18}O_{seawater} = -0.27 \times SST(°C) + 3.22 \tag{8}$$

with N = 5 and R^2 = 0.96.
As $\delta^{18}O_{seawater}$ = 1.29 vs. SMOW = 1.02 vs. PDB was constant, the calibration might be expressed as:

$$\delta^{18}O_{coral} = -0.27 \times SST(°C) + 5.41 \tag{9}$$

4.2 Test of light intensity

Heterotrophy and photosynthesis were linked and were difficult to separate in field experiments. Coral cultures enabled the investigation of each parameter at a time [34, 46].

Tips from 24 branches were sampled from a single parent colony of *Acropora sp*. All colonies were cultured for 6 weeks under a light intensity of 130 µmol m^{-2} s^{-1}. The ring skeleton deposited on the glass slide was then removed with a scalpel [38] dried overnight at room temperature and stored in glass containers pending isotopic analyses. Thereafter, colonies were cultured for an additional period of 6 weeks under a light intensity of 260 µmol m^{-2} s^{-1}, and their isotopic composition

was determined (**Figure 5d**). The extension of new aragonite on the glass slide was assimilated to linear extension.

In the first time [46], the averaged results showed that daily calcification, net photosynthesis significantly increased with increasing light and skeletal $\delta^{18}O_{coral}$ were more negative under low light than high light, −4.2 versus −3.8.

Another interpretation, considering each colony was later published [34]. Following the evolution, $\delta^{13}C_{coral}$ increasing or decreasing, two populations appeared: one responding to light with increasing net photosynthesis associated to low linear extension and the other characterised by poor net photosynthesis associated to high linear extension (**Figure 5d**).

We suggested that different behaviours were due to different zooxanthellae amounts contained by colonies.

4.3 Factorial design of three temperatures and two light intensities

Conditions applied to each tank were referred in the following as (light in μmol photons m^{-2} s^{-1}, temperature in °C): (200, 22), (200, 25), (200, 28), (400, 22), (400, 25) and (400, 28) [15, 48].

Culture procedures are similar to what was described in **Figure 5a** and **b**. Responses of photosynthesis and zooxanthellae density are displayed in **Figure 2**.

Calibrations calculated from the mean $\delta^{18}O$ values for each temperature regime were consistent with those previously published (**Figure 2c**) [49, 50]. $\delta^{18}O$ *versus* temperature calibrations of nubbins cultured under LL and HL were both highly significant (R^2 = 0.94, N = 18, P = 0.001 and R = 0.96, N = 18, P = 0.001, respectively). The slope value was in good agreement with Eq. (2) commonly used for *Porites* corals with b = −0.20‰/°C [37, 51, 52]. However, the values obtained at 22, 25 and 28°C showed a large scattering both at LL and HL, from 0.5 to 1.25‰ or the equivalent of 2 to 5°C.

By comparing our results with other culture experiments [51–53], differences appeared between various $\delta^{18}O$-temperature (°C) calibrations regarding both the slopes and the intercepts with the temperature scale. We suggested that this could be due to inter-species or inter-colony $\delta^{18}O$ differences. Even two calibrations obtained on cultured *Acropora* exhibited differences (the present study and that of Reynaud et al.) [52].

Mean $\delta^{18}O$ values calculated for each temperature did not vary with light, which contradicted observations made of mean physiological parameters, in contrast with other proxies ($\delta^{13}C$, Sr/Ca and Mg/Ca). By changing the light intensity from low to moderate, Juillet-Leclerc and Reynaud [47] recorded a $\delta^{18}O$ increase associated with skeletal infilling following a kinetic process. The present experiment, conducted under high light intensities, did not show a similar behaviour. We suggested that temperature and light effects on isotopic composition were competing. The results of the present experiment indicated that, under the chosen conditions, the temperature effect was more important than the light effect. This was illustrated by the weak discrepancy in the mean $\delta^{18}O$ recorded at 28°C.

Previous culture experiments have been conducted to test the temperature effect on $\delta^{18}O$ [38, 51–54]. Due to the sensitivity of the photosynthesis to temperature, $\delta^{18}O$-temperature calibrations will always include temperature-dependent photosynthetic changes, enabling the vital effect due to temperature only to be deconvolved from the total signature. Therefore, all calibrations, even established on a single coral head or from cultured nubbins, are impacted by photosynthetic activity linked to zooxanthellae density. The universal calibration does not exist.

5. A new paradigm for $\delta^{18}O$ in coral skeleton oxygen isotope fractionation response to biological kinetic effects

During the last experiment, we failed understanding the light effect on $\delta^{18}O$. We kept one colony cultured in each of six light and temperature conditions previously discussed. Knowing that standard error obtained in the first step of the experiment for six samples cultured in the same condition was between 0.02 and 0.12, we consider that values measured on one colony by using SIMS were representative for each environmental condition [48].

We discussed our results after listing all biological and biological advances, such as (i) conclusions derived from inorganic $CaCO_3$ precipitation disturbed by biology, biased by non-realistic models [8, 55, 56]; (ii) the potential role of the calicoblastic layer composed of proteins, sugars and water [57, 58] and (iii) the role of carbonic anhydrase (CA), ubiquitous enzymes known to act as catalysts for the interconversion of CO_2 and HCO_3^- [59, 60].

5.1 Material

The random SIMS measurements were made exclusively on the newly formed skeleton coenosteum (the skeleton portion separating corallites), avoiding newly formed corallites and spines [21]. Samples were distributed along the growth axis from the initial branch to the rim of the expanded tissue (**Figure 7a**).

Measurements were performed using the Cameca IMS 1280-HR ion microprobe at the CRPG, and the comparison of SIMS and conventional mass spectrometer measurements were made using data from [29, 48].

The $\delta^{18}O$ SIMS measurements are displayed as histograms, with bin width of histograms, 0.25‰, depending on the precision of the measurements between 0.09 and 0.32‰ (1σ) (**Figure 7b**).

5.2 Isotopic results

At 22°C, although the mean values were identical within the analytical error, light had a significant effect on the $\delta^{18}O$ distribution. Under LL, the single high bar was surrounded by values spread over 2‰ (**Figure 7b**). By contrast, under HL, values spread over 4‰, $\delta^{18}O$ distribution was bimodal, two high bars were observed, one bar centred on −0.01‰, followed by decreasing values that exceeded the expected $\delta^{18}O$ values for aragonite precipitated in oxygen isotope equilibrium in water.

At 25°C, the bimodal $\delta^{18}O$ distribution in the two samples exhibited two high bars, with the more depleted in ^{18}O peak being the same in the two light conditions (**Figure 7b**).

At 28°C, $\delta^{18}O$ distribution was bimodal, the isotopic amplitude being slightly higher under LL than under HL (**Figure 7b**).

Assuming that two high bars observed in histograms were significant, we used Ashman's D test [61] to strengthen the bimodality of the LL-25°C, LL-28°C, HL-25°C and HL-28°C.

5.3 Discussion

The histograms showed bimodal distributions (except for the colony grown in LL-22°C) caused by distinct kinetic processes. All the colonies were submitted to the diurnal cycle of 12 h light and 12 h dark necessary to grow healthy coral. Therefore, we assumed that, for the high isotopic bar corresponding to the values more depleted in ^{18}O (**Figure 2g**), corresponding to the highest kinetic
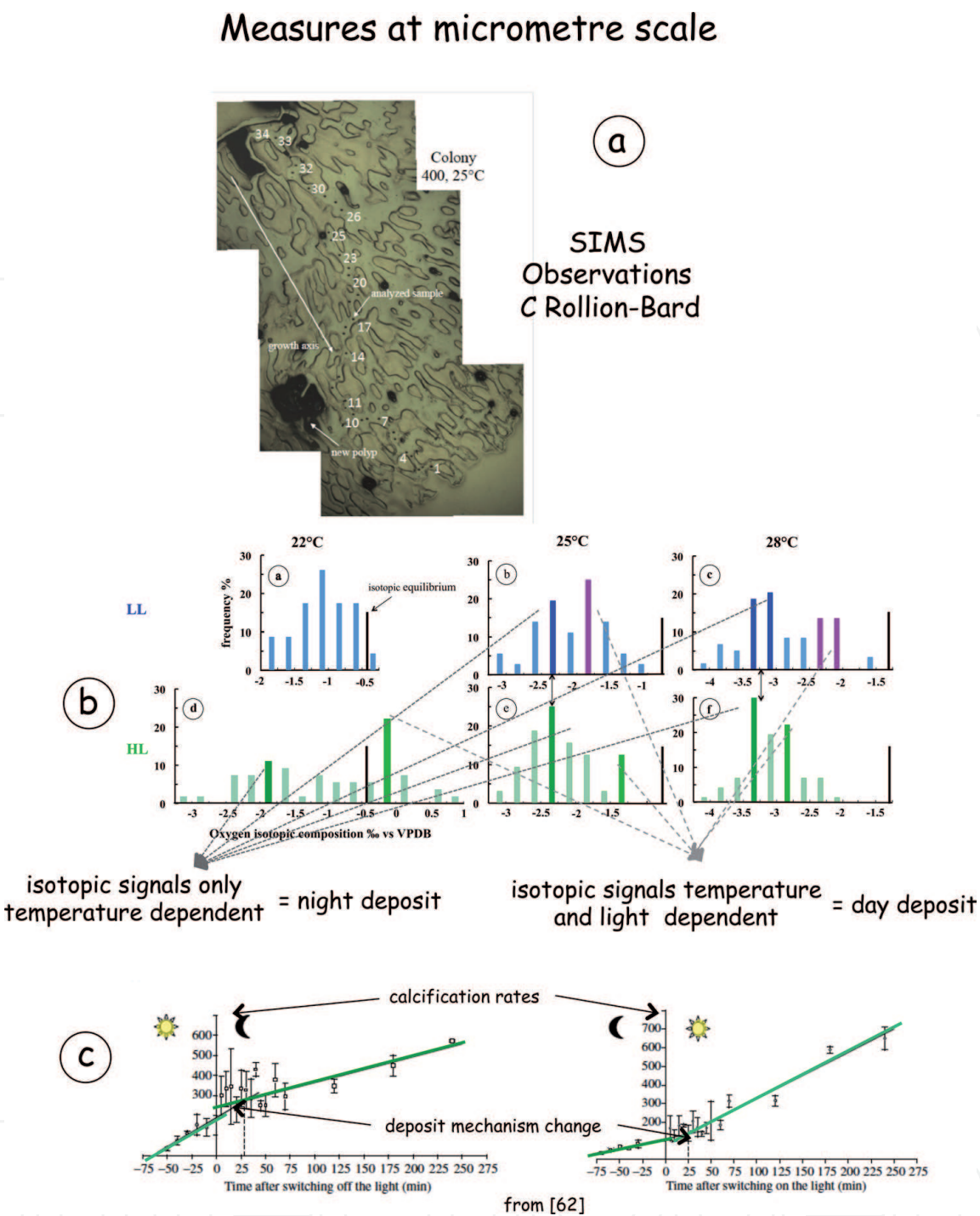
Figure 7.
Test using a factorial design of three temperatures (22, 25, and 28°C) and two light intensities (200 and 400 µmol photon m^{-2} s^{-1}) of cultured Acropora. *SIMS observations of sampling of microscopic scale analyses (a). Isotopic responses displayed as histograms for each environmental conditions showing bimodal distribution (b) corresponding to nighttime and daytime calcification [58] (c).*

fractionation, only depending on temperature is associated with nighttime. By contrast, for the other high isotopic bar corresponding to the values less depleted in ^{18}O, in turn to the weakest kinetic process, depending both on temperature and light could be associated with daytime calcification (**Figure 7b** and **c**).

By culturing *Stylophora pistillata* in controlled conditions similar to those in our experiment [62] with a diurnal cycle of 12 h light and 12 h dark, the authors measured calcification and observed that the calcification rate differed according to night and day conditions (**Figure 7b** and **c**). The regressions showed that the light calcification rate was about 2.4 times higher than the dark calcification rate (**Figure 7c**). However, when conditions shifted from light to dark or from dark to light, the calcification

rate experienced a lag of 25 min between the dark or light regression relative to time (**Figure 7c**). The lag was likely due to the change of calcification process, which differed between nighttime and daytime. These biological evidences were in good agreement with our biochemical ones (**Figure 7b** and **c**). Two assumptions are proposed to explain such a mechanism: a pH change in the extracellular calcifying medium (ECM) and a modification of the biochemical compounds of the organic matrix [62].

Therefore, assuming that the dual high $\delta^{18}O$ bars exhibited in the histograms (**Figure 7b**) were related to the Ca^{2+}-pump activity, this could modify the internal pH [62, 63]. If the pH is lower in the dark than in the light [62, 63], in line with McCrea's [65] calculations, illustrated by Adkins et al. [52], high $\delta^{18}O$ bars less depleted in ^{18}O should be associated with nighttime calcification, and high $\delta^{18}O$ bars more depleted in ^{18}O should correspond to daytime conditions (**Figure 7b** and **c**).

However, our experiment demonstrated an opposite distribution: High $\delta^{18}O$ bars less depleted in ^{18}O were identified as daytime skeleton deposits, and those more depleted in ^{18}O were identified as nighttime deposits. Therefore, we concluded that the two distinct high $\delta^{18}O$ bars could not be caused by internal pH diurnal variations. In contrary to the common assumption [9], we demonstrated that mineralisation is not controlled by classical thermodynamic rules, that is, pH, but rather should obey biological kinetic effects, following a mechanism that remains to be identified.

Now we need to identify a mechanism that allowed daytime and nighttime mineralisation to be distinguished, knowing that the second assumption given by Moya et al. [62], a modification of the biochemical compounds of the organic matrix, remained to be examined.

5.4 Influence of organic matter on crystallisation

It was supposed that the photosynthetic supply of precursors might modify the biochemical composition of an organic matrix [62], which necessitated an internal rearrangement related to the secretion of specific proteins defending the observed lag. The formation of the organic matrix, controlled by the calicoblastic cells, appeared to be a prerequisite for crystallisation [58–67] Recently, 36 proteins were extracted from the skeletal organic matrix (SOM) embedded within aragonite crystals, constituting a bio mineralisation toolkit including at least two Carbonate Anhydrase [68] accelerating mineralisation. From this toolkit, four unique proteins, coral acid-rich proteins (CARP), catalysed the precipitation of $CaCO_3$ in vitro [68]. Moreover, some proteins appeared to be differentially expressed between day and night [68, 69]. Therefore, the two different proteins caused different kinetic fractionation processes, inducing during the night higher kinetic isotope fractionation than during the day. We note that calcification rate and isotope fractionation kinetics were drastically different concepts.

Results derived from our last geochemical experiment should drove to responses also addressed by biological study. The fact that classical geochemistry rule, such as pH, could not explain isotopic behaviour led to look for another assumption. Therefore, it highlighted that coral mineralisation could be controlled by proteins secreted by organic matrix. This evidence is now well admitted, supported by multiple biological studies [68, 69].

6. Simple models

6.1 Model according to microstructure distribution

As early as 1982, Gladfelter [39] assumed that linear extension and infilling were two independent growth rates, an assumption supported by Juillet-Leclerc and

Reynaud [47]. The authors demonstrated that each growth rate was related to preferential deposition of microstructures, COCs ensuring linear extension and fibres, infilling.

Furthermore, geochemical investigations revealed that crystal isotopic signatures differed [27–29, 48]. COC formation should be related to temperature [39] and fibre deposit depends on both temperature and light [48]. Therefore, temperature and light changes interplayed to determine skeletal isotopic composition.

Sampling conducted as it was described by DeLong et al. [40] included both COCs and fibres. Changes of relative amounts of microstructure as illustrated by X-rays and their respective $\delta^{18}O$ were determined by their mechanisms of formation, unknown so far [29]. Following isotopic laws, the combination of calcification processes and isotopic fractionation could be expressed as:

$$\text{measured } \delta^{18}O = \left[\left(x_{COC} \times \delta^{18}O_{COC}\right) + \left(x_{fibre} \times \delta^{18}O_{fibre}\right)\right] / \left(x_{COC} + x_{fibre}\right) \quad (10)$$

where x_{COC} and x_{fibre} are the relative amounts of the crystal microstructures, with $x_{COC} + x_{fibre} = 1$, and $\delta^{18}O_{COC}$ and $\delta^{18}O_{fibre}$ are their isotopic signatures depending on temperature and temperature and light, respectively. This expression is likely to be simplistic but closer to the truth than the thermodynamic formula. Temperature is the prominent factor because included both in the crystal amounts and the isotopic signatures. $SST_{intersection}$, the corresponding $\delta^{18}O_{intersection}$, should be related to morphology [22]. When using Eq. (10), the intersection of calibration should be obtained when $\delta^{18}O_{intersection} = (0.50 \times \delta^{18}O_{COC}) + (0.50 \times \delta^{18}O_{fibre})$ or at $SST_{intersection}$, $\delta^{18}O_{intersection} = (\delta^{18}O_{COC} + \delta^{18}O_{fibre})/2$. As long as temperature does not reach $SST_{intersection}$, more fibres are formed in the coral skeleton and when temperature exceeds $SST_{intersection}$, COC are progressively prevailing.

6.2 Model according to environmental parameters

In Pacific Ocean, local zones may be characterised by seasonal and/or interannual environmental parameter amplitude, as ΔSST. By this way, we are able to identify El Niño-Southern Oscillation (ENSO) occurrence [70], over past time.

$\Delta SST < 2°C$, seasonal conditions occurring in Tarawa atoll, in Galapagos or in Fiji [71], $\delta^{18}O$ seasonal variability mimics SSS variability. In Fiji, $\delta^{18}O$ is correlated to seasonal precipitation [72]. In other sites, $\delta^{18}O$ variability may indicate oceanic advection. Such events are directly related to El Niño.

If seasonal $\delta^{18}O$ is recorded over several decades, interannual variability may be isolated. By removing the seasonal cycle and applying a 13-month running mean filter from monthly $\delta^{18}O$, interannual isotopic variability may be regarded as temperature, the greatest fluctuations revealing El Niño-Southern Oscillation (ENSO) occurrence [70], or the global warming over the twentieth and twenty-first century.

When $\Delta SST \geq 5°C$, as it is occurring off South Korea coast [72], temperature and $\delta^{18}O_{seawater}$ are both involved in coral skeleton $\delta^{18}O$ variability. Environmental parameters are difficult to separate. If $\delta^{18}O$ shows strong decrease associated to great SST drops, it may be caused by the occurrence of La Niña (characterised by colder SST than the normal conditions) [70].

When $2°C \leq \Delta SST \leq 4°C$ as it is recorded in the central tropical Pacific as in Palmyra [73], $\delta^{18}O$ snapshots focused on crucial past periods demonstrate that a 2- to 7-yr bandpassed record (the lower-frequency of ENSO) [70], the interannual isotopic signal highlights El Niño and La Niña occurrences.

Coral skeletal $\delta^{18}O$ is well-suited tool to shed in light climatic events before and after industrial era, to predict future events in the next decades [70].

7. Conclusion

Coral skeleton $\delta^{18}O$ does not obey to classical thermodynamics but rather reflects aragonite microstructure distribution. We demonstrated that oxygen isotopic fractionation is essentially temperature dependent, due to two temperature effects, one following thermodynamic law, decreasing $\delta^{18}O$ when temperature increases, and second, temperature acting through photosynthetic process, increasing $\delta^{18}O$ when temperature increases. Consequently, when temperature changes, $\delta^{18}O$ is affected in opposite senses, confusing the global isotopic effect.

$\delta^{18}O$ measured at millimetre size scale on coral colonies cultured in controlled conditions under varying temperatures and/or light intensities, allows highlighting biologic and isotopic changes associated to environmental factors, acting as vital effect. Measured at microscopic size, $\delta^{18}O$ reveals mineralisation processes. By using the last method coupled with biologic evidences, the role of proteins and enzymes, secreted by organic matrix at the interface tissue mineral is demonstrated, showing the potential biologic control on meralisation.

Author details

Anne Juillet-Leclerc
LSCE, Gif sur Yvette, France

*Address all correspondence to: anne.juillet-leclerc@lsce.ipsl.fr

IntechOpen

References

[1] Allemand D, Ferrier-Pagès C, Furla P, Houlbrèque F, Puverel S, Reynaud S, et al. Biomineralisation in reef-building corals: From molecular mechanisms to environmental control. General Palaeontology (Palaeobiochemistry) Comptes Rendus Palevol. 2004;**3**:453-467

[2] Salvat B. Le corail et les récifs coralliens. Ouest France: Découverte Nature Ed; 2003

[3] Weber JN, Woodhead PMJ. Temperature dependence of oxygen-18 concentration in reef coral carbonates. Journal of Geophysical Research. 1972;**77**:463-473

[4] Epstein S, Buchsbaum R, Lowenstam H, Urey HC. Carbonate water isotopic temperature scale. Bulletin Geological Society of America. 1951;**62**:417

[5] Epstein S, Buchsbaum R, Lowenstam H, Urey HC. Revised carbonate-water isotopic temperature scale. Bulletin Geological Society of America. 1953;**62**:417-425

[6] Weber JN, Woodhead PMJ. Ecological studies of the coral predator *Acanthaster planci* in the South Pacific. Marine Biology. 1970;**6**:12-17

[7] McConnaughey TA. C-13 and O-18 isotopic desequilibrium in biological carbonates: I. Patterns. Geochimica et Cosmochimica Acta. 1989;**53**:151-162

[8] McConnauguey TA. C-13 and O-18 isotopic disequilibria in biological carbonates: II. In vitro simulation of kinetic isotope effects. Geochimica et Cosmochimica Acta. 1989;**53**:163-171

[9] Cohen A, McConnaughey TA. Geochemical perspectives on coral mineralization reviews in mineralogy and geochemistry. In: Dove PM, de Yoreo JJ, Weiner S, editors. Biomineralization. Vol. 54. Mineralogical Society of America; 2003. pp. 151-187

[10] Gaetani GA, Cohen AL. Element partitioning during precipitation of aragonite from seawater: A framework for understanding paleoproxies. Geochimica et Cosmochimica Acta. 2006;**70**:4617-4634

[11] Cohen AL, Gaetani GA, Lundälv T, Corliss BH, George RY. Compositional variability in the cold-water scleractinian, *Lophelia pertusa*: New insights into "vital" effects. Geochemistry, Geophysics, Geosystems. 2006;**7**. DOI: 10.1029/2006GC001354

[12] Gagnon AC, Adkins JF, Fernandez DP, Robinson LF. Sr/Ca and Mg/Ca vital effects correlated with skeletal architecture in a scleractinian deep-sea coral and the role of Rayleigh fractionation. Earth and Planetary Science Letters. 2007;**261**:280-295

[13] Gaetani GA, Cohen AL, Wang Z, Crusius J. Rayleigh-based, multi-element coral thermometry: A biomineralization approach to developing climate proxies. Geochimica et Cosmochimica Acta. 2011;**75**:1920-1932. DOI: 10.1016/j.gca.2011.01.010

[14] Veron JEN. Corals of Australia and the Indo-Pacific. University of Hawaii Press; 1986

[15] Juillet-Leclerc A, Reynaud S, Dissard D, Tisserand G, Ferrier-Pagès C. Light is an active contributor to vital effects of coral skeleton proxies. Geochimica et Cosmochimica Acta. 2014;**140**:671-690

[16] Barnes DJ, Chalker BE. Calcification and photosynthesis in reef-building corals and algae. In: Dubinsky Z, editor. Coral Reefs. Ecosystems of the World. Vol. 25. Amsterdam: Elsevier; 1990. pp. 109-131

[17] Iluz D, Dubinski D. Coral photobiology: New light on old views. Zoologica. 2015;**118**:71-78

[18] Von Euw S, Zhang Q, Manichev V, Murali N, Gross J, Feldman LC, et al. Biological control of aragonite formation in stony corals. Science. 2017;**356**:933-938

[19] Cuif JP, Dauphin Y. Microstructural and physico-chemical characterisation of centres of calcification in septa of some scleractinian corals. Palaeontologische Zeitschrift. 1998;**72**:257-270

[20] Stolarski J. Three-dimensional micro- and nanostructural characteristics of the scleractinian coral skeleton: A biocalcification proxy. Acta Palaeontologica Polonica. 2003;**48**:497-530

[21] Nothdurft LD, Webb GE. Microstructure of common reef-building coral genera *Acropora*, *Pocillopora*, *Goniastrea* and *Porites*: Constraints on spatial resolution in geochemical sampling. Facies. 2007;**53**:1-26

[22] Land LS, Lang JC, Barnes DJ. Extension rate: A primary control on the isotopic composition of west Indian (Jamaican) scleractinian reef coral skeletons. Marine Biology. 1975;**3**:221-233

[23] Zinke J, Rountrey A, Feng M, Xie SP, Dissard D, Rankenburg K, et al. Corals record long-term Leeuwin current variability including Ningaloo Niño/Niña since 1795. Nature Communications. 2014. DOI: 10.1038/ncomms4607

[24] Tierney JE, Abram NJ, Anchukaitis KJ, Evans MN, Giry C, Kilbourne KH, et al. Tropical Sea surface temperatures for the past four centuries reconstructed from coral archives. Paleoceanography. 2015. DOI: 10.1002/2014PA002717

[25] Wu HC, Linsley BK, Dassié EP, Schiraldi B Jr, de Menocal BP. Oceanographic variability in the South Pacific convergence zone region over the last 210 years from multi-site coral Sr/Ca records. Geochemistry, Geophysics, Geosystems. 2013. DOI: 10.1029/2012GC004293

[26] Gattuso JP, Allemand D, Frankignoulle M. Photosynthesis and calcification at cellular, organismal and community levels in coral reefs: A review on interactions and control by carbonate chemistry. American Zoologist. 1999;**39**:160-183

[27] Rollion-Bard C, Chaussidon M, France-Lanord C. pH control on oxygen isotopic composition of symbiotic corals. Earth Plan Scence Review. 2003;**215**:265-273

[28] Meibom A, Yurimoto H, Cuif JP, Domart-Coulon I, Houlbrèque F, Constantz B, et al. Vital effect in coral skeletal composition display strict three-dimensional control. Geophysical Research Letters. 2006;**30**. DOI: 10.1029/2006GL025968

[29] Juillet-Leclerc A, Reynaud S, Rollion-Bard C, Cuif JP, Dauphin Y, Blamart D, et al. Oxygen isotopic signature of the skeletal microstructures in cultured corals: Identification of vital effects. Geochimica et Cosmochimica Acta. 2009;**73**:5320-5332

[30] Urey HC. Thermodynamic properties of isotopic substances. Journal of the Chemical Society. 1947:562-581

[31] Barnes DJ, Lough JM. Coral skeletons: Storage and recovery of environmental information. Global Change Biology. 1996;**2**:569-582

[32] Juillet-Leclerc A, Schmidt G. A calibration of the oxygen isotope paleothermometer of coral aragonite

from *Porites*. Geophysical Research Letters. 2001;**28**:4135-4138

[33] Kim ST, O'Neil JR, Hilaire-Marcel C, Mucci A. Oxygen isotope fractionation between synthetic aragonite and water. Influence of temperature and Mg^{2+} concentration. Geochimica et Cosmochimica Acta. 2007;**71**:4704-4715

[34] Juillet-Leclerc A, Reynaud S. Light effects on the isotopic fractionation of skeletal oxygen and carbon in the cultured zooxanthellate coral, *Acropora*: Implications for coral-growth rates. Biogeosciences. 2010;**7**:893-906

[35] Marshall JF, McCulloch MT. An assessment of the Sr/Ca ratio on shallow water hermatypic corals as a proxy for sea surface temperature. Geochimica et Cosmochimica Acta. 2002;**66**:3263-3280

[36] D'Olivo JP, Sinclair DJ, Rankenburg K, McCulloch MT. A universam multi-trace element calibration for reconstructing sea surface temperatures from long-lived Porites corals: Removing "vital effects". Geochimica et Cosmochimica Acta. 2018;**239**:109-135

[37] Cohen AL, Layne GD, Hart SR, Lobel PS. Kinetic control of skeletal Sr/Ca in a symbiotic coral: Implications for the paleotemperature proxy. Paleoceanography. 2001;**16**:20-26

[38] Reynaud-Vaganay S, Gattuso JP, Cuif JP, Jaubert J, Juillet-Leclerc A. A novel culture technique for scleractinian corals: Application to investigate changes in skeletal $\delta^{18}O$ as a function of temperature. Marine Ecology Progress Series. 1999;**180**:121-130

[39] Gladfelter EH. Skeletal development in *Acropora cervicornis*: I. Patterns of calcium carbonate accretion in the axial corallite. Coral Reefs. 1982;**1**:45-51

[40] DeLong KL, Quinn TM, Taylor FW, Shen CC, Lin K. Improving coral-base paleoclimate reconstructions by replicating 350 years of coral Sr/Ca variations. Palaeogeography, Palaeoclimatology, Palaeoecology. 2013;**373**:6-24

[41] Quinn T, Sampson DE. A multiproxy approach to reconstructing sea surface conditions using coral skeleton geochemistry. Paleoceanography. 2002;**17**:1062. DOI: 10.1029/2000PA000528

[42] Stephans CL, Quinn TM, Taylor FW, Corrège T. Assessing the reproducibility of coral-based climate records. Geophysical Research Letters. 2004;**31**:L18210. DOI: 10.1029/2004GL020343

[43] Linsley BK, Messier RG, Dunbar RB. Assessing between-colony oxygen isotope variability in the coral *Porites lobata* at Clipperton Atoll. Coral Reefs. 1999;**18**:13-27

[44] Maier C, Felis T, Pätzold J, Bak RPM. Effect of skeletal growth and lack of species effects in the skeletal oxygen isotope climate signal within the coral genus *Porites*. Marine Geology. 2004;**207**:93-208

[45] Boiseau M, Juillet-Leclerc A. H_2O_2 treatment of recent coral aragonite: Oxygen and carbon isotopic implications. Chemical Geology. 1997;**143**:171-180

[46] Reynaud-Vaganay S, Juillet-Leclerc A, Gattuso JP, Jaubert J. Effect of light on skeletal $\delta^{13}C$ and $\delta^{18}O$ and interaction with photosynthesis, respiration and calcification in two zooxanthellate scleractinian corals. Palaeogeography, Palaeoclimatology, Palaeoecology. 2001;**175**:393-404

[47] Juillet-Leclerc A, Reynaud S. Light effects on the isotopic fractionation of skeletal oxygen and carbon in the cultured zooxanthellate coral, Acropora: implications for coral-growth rates. Biogeosciences. 2010;**7**:893-906

[48] Juillet-Leclerc A, Rollion-Bard C, Reynaud S, Ferrier-Pagès C. A new paradigm for δ18O in coral skeleton oxygen isotope fractionation response to biological kinetic effects. Chemical Geology. 2018;**483**:131-140

[49] Yu KF, Zhao JX, Wei GJ, Cheng XR, Chen TG, Felis T, et al. $\delta^{18}O$, Sr/Ca and Mg/Ca records of *Porites lutea* corals from Leizhou Peninsula, northern South China Sea, and their applicability as paleoclimatic indicators. Palaeogeography, Palaeoclimatology, Palaeoecology. 2005;**218**:57-73

[50] Corrège T. Sea surface temperature and salinity reconstruction from coral geochemical tracers. Palaeogeography, Palaeoclimatology, Palaeoecology. 2006;**232**:408-428

[51] Inoue M, Suzuki A, Nohara M, Hibino K, Kawahata H. Empirical assessment of coral Sr/Ca and Mg/Ca ratios as climate proxies using colonies grown at different temperatures. Geophysical Research Letters. 2007;**34**:L12611. DOI: 10.1029/2007GL029628

[52] Reynaud S, Ferrier-Pagès C, Meibom A, Mostefaoui S, Mortlock R, Fairbanks R, et al. Light and temperature effects on Sr/Ca and Mg/Ca ratios in the scleractinian coral *Acropora* sp. Geochimica et Cosmochimica Acta. 2007;**71**:354-362

[53] Suzuki A, Hibino K, Iwase A, Kawahata H. Intercolony variability of skeletal oxygen and carbon isotope signatures of cultured *Porites* corals: Temperature-controlled experiments. Geochimica et Cosmochimica Acta. 2005;**69**:4453-4462. DOI: 10.1016/j. gca.2005.05.018

[54] Armid A, Asami R, Fahmiati T, Sheikh MA, Fujimura H, Higuchi T, et al. Seawater temperature proxies based on DSr, DMg, and DU from culture experiments using the branching

coral *Porites cylindrica*. Geochim Cosmochim Acta. 2011;**75**:4273-4285

[55] Adkins JF, Boyle EA, Curry WB, Lutringer A. Stable isotopes in deep-sea corals and a new mechanism for "vital effects". Geochimica et Cosmochimica Acta. 2003;**67**:1129-1143

[56] Gaetani GA, Cohen AL, Wang Z, Crusius J. Rayleigh-Based, Multi-Element Coral Thermometry: a Biomineralization Approach to Developing Climate Proxies. Geochim Cosmochim Acta. 2011;**75**:1920-1932

[57] Bertucci A, Moya A, Tambutté S, Allemand D, Supuran CT, Zoccola D. Carbonic anhydrases in anthozoan corals. A review. Bioorganic & Medicinal Chemistry. 2013;**21**:1437-1450

[58] Mass T, Drake JL, Peters EC, Jiang W, Falkowski PG. Immunolocalization of skeletal matrix proteins in tissue and mineral of the coral *Stylophora pistillata*. Proceedings of the National Academy of Sciences of the United States of America. 2014;**111**:12728-12733

[59] Allemand D, Tambutté E, Zoccola D, Tambutté S. Coral calcification, cells to reefs. In: Dubinski Z, Stambler N, editors. Coral Reefs: An Ecosystem in Transition. Springer Science + Business Media; 2011. pp. 119-150

[60] Uchikawa J, Zeebe RE. The effect of carbonic anhydrase on the kinetics and equilibrium of the oxygen isotope exchange in the CO_2-H_2O system: Implications for $\delta^{18}O$ vital effects in biogenic carbonates. Geochimica et Cosmochimica Acta. 2012;**95**:15-34

[61] Ashman KM, Bird CM, Zepf SE. Detecting bimodality in astronomical datasets. Astronomy Journal. 1994;**108**. DOI: 10.1086/117248

[62] Moya A, Tambutté S, Tambutté E, Zoccola D, Caminiti N,

Allemand D. Study of calcification during a daily cycle of the coral *Stylophora pistillata*: Implications for light-enhanced calcification. The Journal of Experimental Biology. 2006;**209**:3413-3419

[63] Puverel S, Tambutté É, Pereira-Mouries L, Zoccola D, Allemand D, Tambutté S. Soluble organic matrix of two scleractinian corals: Partial and comparative analysis. Comparative Biochemistry and Physiology. 2005;**141B**:480-487

[64] Moya A, Tambutté S, Lotto S, Allemand D, Zoccola D. Carbonic anhydrase in the scleractinian coral *Stylophora pistillata*: Characterization, localization, and role in biomineralization. The Journal of Biological Chemistry. 2008;**283**:25475-25484

[65] McCrea JM. On the isotopic chemistry of carbonates and a paleotemperature scale. The Journal of Chemical Physics. 1950;**18**:849-857

[66] Al-Horani FA, Al-Moghrabi SM, de Beer D. The mechanism of calcification and its relation to photosynthesis and respiration in the scleractinian coral *Galaxea fascicularis*. Marine Biology. 2003;**142**:419-426

[67] Venn AA, Tambutté É, Holcomb M, Allemand D, Tambutté S. Live tissue imaging shows reef corals elevate pH under their calcifying tissue relative to seawater. PLoS One. 2011;**6**(5):e20013

[68] Mass T, Drake JL, Haramaty L, Kim JD, Zelzion E, Bhattacharya D, et al. Cloning and characterization of four novel coral acid-rich proteins that precipitate carbonates *In Vitro*. Current Biology. 2013;**23**:1126-1131

[69] Bertucci A, Forêt S, Ball EE, Miller DJ. Transcriptomic differences between day and night in *Acropora millepora* provide new insights into

metabolite exchange and light-enhanced calcification in corals. Molecular Ecology. 2015;**24**:4489-4504

[70] Cai W, Borlace S, Lengaigne M, van Rensch P, Collins M, Vecchi G, et al. Increasing frequency of extreme El Niño eventsdue to greenhouse warming. Nature Climate Change. 2014;**4**:111-116

[71] Le Bec N, Juillet-Leclerc A, Correge T, Blamart D, Delcroix T. A coral δ^{18}O record of ENSO driven sea surface salinity in Fiji (south-western tropical Pacific). Geophysical Research Letters. 2000;**27**:3897-3900

[72] Shimamura M, Hyeong K, Yoo CM, Watanabe T, Irino T, Jung HS, et al. High resolution stable isotope records of sclreractinian corals near Ishigaki Island: Their implication as a potential paleoclimatic recorder in middle latitude regions. Geosciences Journal. 2008;**12**:25-31

[73] Cobb KM, Charles CD, Cheng HR, Edwards L. El Niño/southern oscillation and tropical Pacific climate during the last millennium. Nature. 2003;**424**:271-276